Research Article Vol. 28, No. 5 / 2 March 2020 / Optics Express 7108
Optics EXPRESS

High power femtosecond semiconductor lasers based on saw-toothed master-oscillator power-amplifier system with compressed ASE

YANJING WANG,[1,2] XIN ZHANG,[1,2] CUNZHU TONG,[1,*] LIJIE WANG,[1] SHILI SHU,[1] SICONG TIAN,[1] AND LIJUN WANG[1]

[1] *State Key Laboratory of Luminescence and Applications, Changchun Institute of Optics, Fine Mechanics and Physics, Chinese Academy of Sciences, Changchun 130033, China*
[2] *Center of Materials Science and Optoelectronics Engineering, University of Chinese Academy of Sciences, Beijing 100049, China*
[*] *tongcz@ciomp.ac.cn*

Abstract: High power femtosecond semiconductor laser based on saw-toothed taper mode-locked laser and amplifier was demonstrated with compressed amplified spontaneous emission (ASE). The external-cavity mode-locked taper laser generated the clean optical pulses without any sub-pulse components. A semiconductor optical amplifier (SOA) with tilted taper waveguide and saw-toothed edge reduced evidently the ASE background. The saw-tooth microstructures were optimized and it was found that the saw-tooth of right-right angled triangle showed the best effect. The ratio of the maximum intensity to background radiation was increased by 21.9% and the power was increased by 30.5% due to the saw-tooth microstructure in the SOA. The pulse duration of 495 fs and a peak power over 1.5 kW with repetition rate of 579 MHz were realized after a double-pass grating compressor.

1. Introduction

In recent years, the demand for lasers generating high-power femtosecond optical pulses is increasing significantly. Such lasers are widely used for precision processing of materials [1–4], super-continuum generation [5–8], parametric oscillators pumping [9,10], and multiphoton imaging [11–13]. The pulse energies of several hundreds of picojoules and peak powers up to multi-watts emitted by single pulse diode lasers are often not sufficient for most applications. Higher peak powers can be obtained by amplification of the pulses with master oscillator-power amplifier (MOPA) systems [14–17]. However, for the power amplifiers (PA), most of the emitted power consists of amplified spontaneous emission (ASE). A high ASE intensity leads to a reduction in excited carriers in the conduction/valence bands through the stimulated emission process which limits the amplification rate [18].

The electrical coupling between the two pulse generators for master oscillator (MO) and PA [19,20] is a recently developed technique, which has been used to reduce the ASE and improve the powers of a MOPA system. The PA is driven by short electrical pulses to reduce the ASE among the pulses. In 2011, S. Schwertfeger et al. [19] demonstrated a peak power of 50 W using a MO of Q-switching laser diode and a PA in pulse operation. The ASE power was reduced to values below 18% of the total emitted power. In 2013, a gain-switching laser diode was used as MO and achieved a peak power of more than 65 W [20]. However, this method is only suitable for the case of Q-switching or gain-switching laser diode as MO. In addition, the Q-switching and gain-switching laser diode usually has longer pulse duration (typically 10 ps to 100 ps) and is difficult for high peak power operation.

In this work, we propose an all-semiconductor femtosecond MOPA system with saw-toothed microstructures. The generation of clean optical pulses was achieved from an external-cavity

#385576 https://doi.org/10.1364/OE.385576
Journal © 2020 Received 23 Dec 2019; revised 28 Jan 2020; accepted 7 Feb 2020; published 25 Feb 2020

Optics EXPRESS

mode-locked oscillator and the ASE in the tapered semiconductor optical amplifier (SOA) was significantly reduced using saw-toothed microstructures. The mechanism behind was presented. Finally, femtosecond pulses were realized and the pulse characteristics and lasing spectra were analyzed.

2. Experimental setup

A scheme of the MOPA setup is shown in Fig. 1. The MOPA system mainly consists of an external cavity mode-locked laser (ECMLL), a tapered SOA and a double-pass grating compressor. Picosecond optical pulses were generated by an ECML with tapered gain waveguide and then passed through an optical isolator (OI). A half-wave ($\lambda/2$) plate was used to obtain the maximum SOA gain with TE polarized input light. At the end of the half-wave plate, an aspheric lens with focal length of 4.5 mm was used to focus light into the tapered waveguide of SOA, which was a tilted cavity with saw-toothed edge. The input and output facets were anti-reflection (AR) coating with reflectivity less than 0.5%. After amplification of these picosecond pulses, an aspheric lens with 3.1 mm focal length and a cylindrical lens with 25 mm focal length were used to collimate the beam in fast and slow axes, respectively. Then the pulses entered a double-pass pulse compressor and the duration was compressed to the femtosecond range.

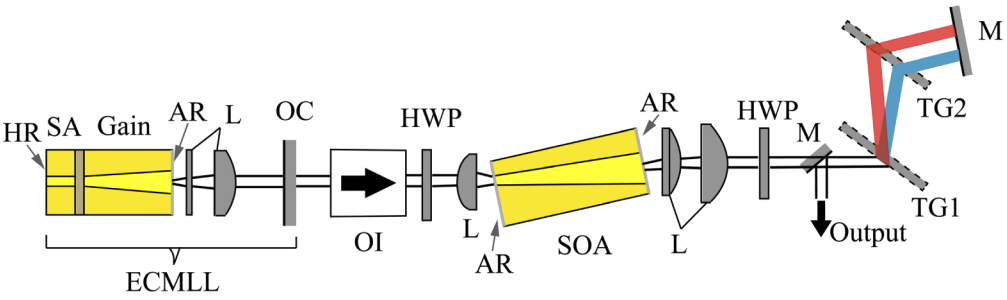

Fig. 1. Schematic diagram of the femtosecond MOPA semiconductor laser system. ECMLL: external cavity mode-locked laser, SA: saturable absorber, HR: high-reflection coating, AR: anti-reflection coating, L: collimating lenses, OC: output coupler (63%), OI: optical isolator, HWP: half-wave plate, M: mirror, TG: transmission grating.

A power meter PM100D from Thorlabs was used to measure the average power. The autocorrelation trace was recorded by an intensity autocorrelator Pulse Check 1200, which offers a scan range from 120 fs to 300 ps. The optical spectra were measured using the grating spectrometer AQ6370B from Yokogawa with a resolution $\Delta\lambda = 0.05$ nm. A fast photodiode DET08C from Thorlabs and a radio frequency spectrum analyzer MDO3104 from Tektronix were used to characteristic the repetition rate of mode-locked laser.

3. Mode-locked master oscillator

The MO is an external-cavity mode-locking (ECMLL) tapered waveguide laser with saw-toothed microstructure. The total length of the external cavity was 23.5 cm. Two spherical cylindrical lenses with focal lengths of 0.36 mm and 7.5 mm were used to collimate the beam in slow and fast axes, respectively. An output coupler (OC) with transmissivity of 63% was used to supply the external cavity feedback. The total length of the fabricated taper mode-locked laser was 3020 μm, which included a saturable absorber (SA) section and a tapered gain section. The SA section was 120 μm long and 5 μm wide ridge waveguide. The tapered gain section had a full -flare angle of 3 degrees and a length of 2885 μm. The shape of the side-wall saw-toothed microstructure is a right triangle with a length of 3 μm and a height of 2.5 μm. The waveguide and saw-toothed

Optics EXPRESS

microstructure were first fabricated using inductively coupled plasma (ICP) etching with a depth of 1.5 μm. The AR coating of < 0.5% and high-reflection (HR) coating of 98% were respectively deposited at the front and rear facet. The details of the device structure can be found in our previous work [21].

The epitaxial structure of MO device was a typical asymmetric super-large optical cavity (SLOC) and was grown by metal organic chemical vapor deposition (MOCVD) on n+ GaAs substrate. The SLOC consisted of 3.0 μm and 1.2 μm n- and p-type doped AlGaAs waveguides. The gain material was two InGaAs quantum wells (QWs) with emission wavelength of 965 nm, and embedded in 600 nm and 550 nm $Al_{0.35}Ga_{0.65}As$ cladding layers. The top layer of epitaxial structure is 200 nm heavily doped GaAs for ohmic contact. More details on the epitaxial structure can be found in Ref. [22].

The measured repetition rate of ECMLL was about 579 MHz, the average power was 28 mW at the driven current of 750 mA and SA reverse voltage of 3.4 V. Figure 2(a) shows the autocorrelation trace of the ECMLL pulses. It can be seen that there were no noticeable sub-pulse components accompanying the main pulse. It is worth emphasizing that the generation of clean optical pulses is essential since any distortion of the input pulse would result in the distortion of amplified pulses. The autocorrelation width is 5.8 ps with a near Lorentz shape. The spectrum was showed in Fig. 2(b). The peak wavelength is 965.8 nm and the full-width at half-maximum (FWHM) is 3.6 nm. The shape of spectrum is not symmetric. The longer wavelength edge of the pulse is much steeper than the short wavelength edge. This asymmetry is indeed a result of the strong chirp because the spectral components at the front side of the pulse experience more gain than those at the tail [23]. The time-bandwidth product (TBP) was estimated to be 6.7, implying the MO emitted pulses with a strong chirp.

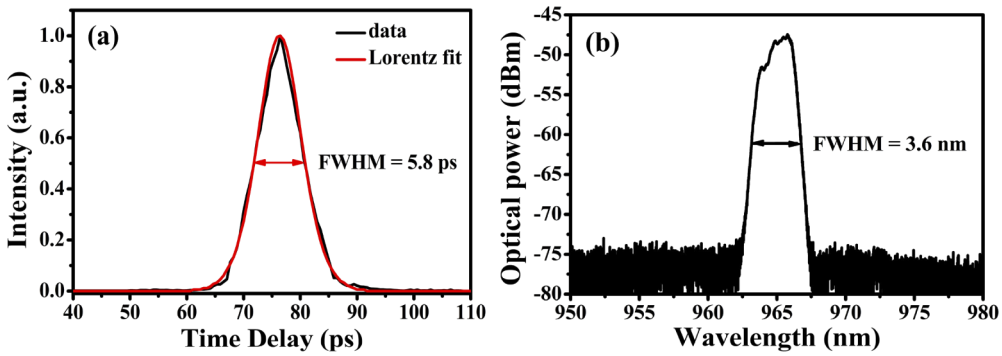

Fig. 2. Autocorrelation trace (a) and optical spectrum (b) of a pulse emitted from the ECMLL at 750 mA gain current and 3.4 V bias voltage of reverse absorber.

4. Pulse amplification

Figure 3(a) shows the structure of tapered SOA with saw-toothed microstructure. The SOA was also grown by MOCVD with the same epitaxial structures as the ECMLL. The total length of the SOA chip was 4.5 mm with a full flare angle of 6 degrees. The waveguide width was changed from 15 μm at the input facet to 493 μm at the output facet. The waveguide and saw-toothed microstructure were firstly fabricated by ICP etching with a depth of 1.7 μm. Then an electrical insulating layer was deposited and contact window opening was performed, followed by p-side Ti–Pt–Au contact metal deposition, substrate thinning, and n-side AuGeNi–Au metal deposition. The tapered waveguide was angled at 7 degrees relative to the central axis of the SOA chip to reduce the facet feedback. Finally, the SOA was mounted on a copper heat sink with n-side down using indium solder. The temperature of SOA was stabilized at 16 °C using a Peltier

Optics EXPRESS

cooler. Figure 3(b) shows the generation of ASE in a conventional amplifier (SOA). Spontaneous emission photons are reflected back to the cavity multiple times to be amplified by the waveguide sidewalls. In contrast, in the SOA having saw-toothed microstructure [Fig. 3(c)], when the photons are incident into the waveguide sidewalls, the saw-toothed microstructure will reflect them out of the cavity. Hence, the spontaneously emitted photons cannot be amplified effectively and the ASE will be compressed.

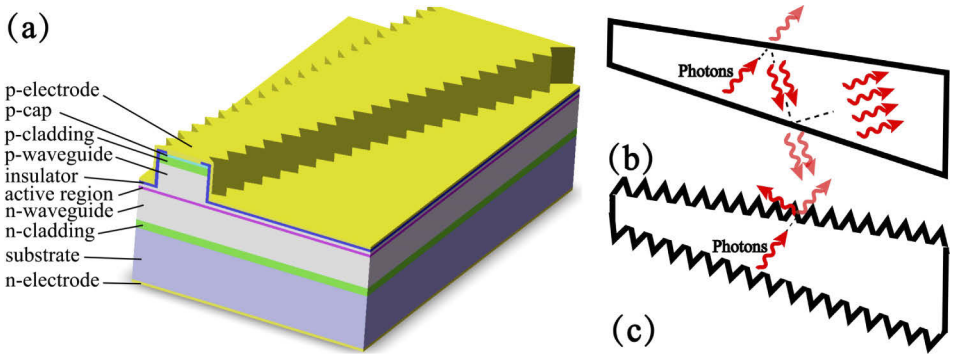

Fig. 3. (a) Schematic diagram of SOA structure, (b) mechanism of ASE in a conventional SOA and (c) compressing ASE in a SOA with saw-toothed edge.

To optimize the saw-toothed microstructure, the SOA device A, B and C with different saw-toothed microstructure were fabricated. The same shape tapered SOA without microstructure (D) is used as contrast. Figure 4 shows the saw-tooth microstructures of right-right angled triangle (A), left-right angled triangle (B), isosceles triangles (C). The corresponding length (L) is 5 μm and height (H) is 5 μm.

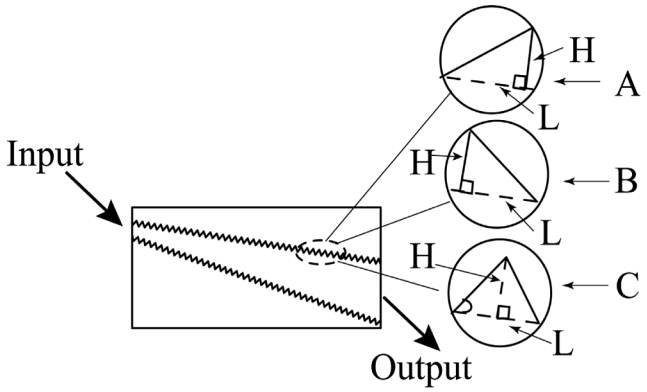

Fig. 4. The saw-toothed microstructure in the tapered SOA.

Figure 5 shows the time-averaged spectra of the amplified pulses from the SOA devices A, B, C, and D at a bias current of 4.6 A. The optical spectra of the conventional device D shows the strong ASE background and the ratio of the maximum intensity to the ASE background is 16.4 dB as showed in Fig. 5(d). In contrast, the device A, B and C with saw-toothed microstructure show the improved ASE background. According to Figs. 5(a), 5(b) and 5(c), the ratio of the maximum intensity to the ASE background for device A, B and C are 20 dB, 18.3 dB and 17.8 dB, respectively. Device A shows the largest compression of ASE. It might be because that the saw-tooth microstructure of right-right angled triangle is more effective to reflect the

Optics EXPRESS

spontaneously emitted photons out of the cavity, and hence decreases the ASE. The ratio of the maximum intensity to background radiation is increased by 21.9%.

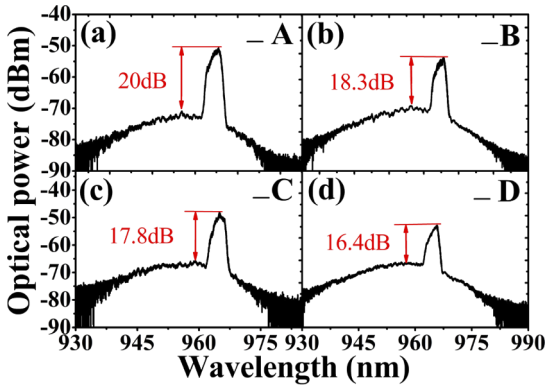

Fig. 5. Optical spectra of amplified pulse with ASE background at SOA current of 4.6 A.

The pulse amplified power from the SOA-A (blue), B (red), C (green), D (black) were plotted in Fig. 6(a) as a function of current. The average power of MO was 28 mW, but the power inputted into the SOA was reduced to 21.3 mW because the coupling optical loss between the ECMLL and SOA. The average power shown in Fig. 6(a) represents the power obtained from the SOA subtracting the power contribution from the broadband ASE, the latter was measured under the condition without the oscillator input. It can be seen that the average power of the SOA with saw-toothed microstructure (device A, B, C) is much higher than that of the conventional device D. When the driven current of SOA is 4.6 A, the power for device A is 799 mW, corresponding to an improvement of 30.5% compared with the power of 612 mW of device D. Figure 6(b) shows the pulse duration as a function of SOA current. The pulse durations of device A, B, C and D are in the range from 6.3 ps to 6.8 ps and show a weak dependence on the driven current.

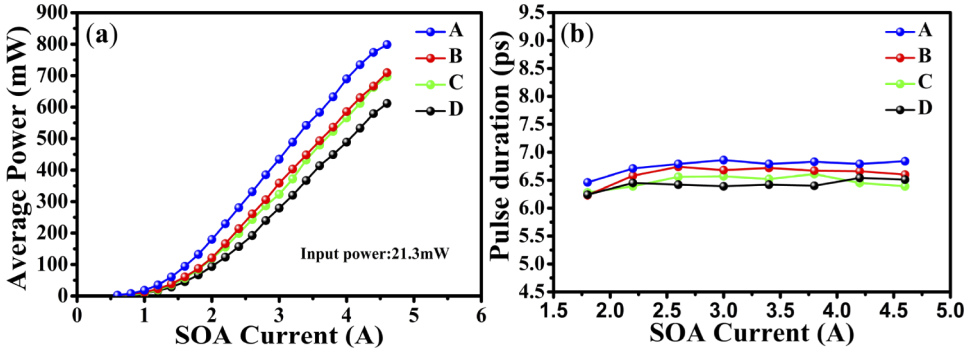

Fig. 6. Average power (a) and pulse duration (b) of the amplified pulses as a function of SOA current.

5. Pulse compression

A double-pass grating compressor was used to compress the pulses from the SOA. Since the beam is reflected twice at each grating, the output power depends strongly on the diffraction efficiency. The used gratings provided a first order diffraction efficiency of 93% and 1850 lines per millimeter. The double-pass grating compressor is able to compensate the group delay

Optics EXPRESS

dispersion (GDD), which can be described as [24]:

$$\mathrm{GDD} = -\frac{\lambda^3}{\pi c^2 d^2}\,\frac{Z}{1-(\frac{\lambda}{d}-\sin\theta)^2}, \tag{1}$$

where λ denotes the center wavelength of the pulse (965 nm), Z is the length of optical path between the gratings. d is the grating groove width (~0.54 μm) and θ is the angle of incidence on the first grating (θ=64°). The value of θ was chose for the purpose of the highest diffraction efficiency of the grating with the first order diffraction. The amount of dispersion can be adjusted by changing Z. The shortest pulse duration was obtained at Z = 20 mm. Hence the estimated GDD is –1.11 ps^2. Figs. 7(a) and 7(b) show respectively the autocorrelation trace of the pulse measured after the amplifier and the pulse compressor for SOA device A and D at the driven current of 4.6 A. As shown in Figs. 7(a) and 7(b), the compressed pulses have a similar pulse shape and almost the same pulse width for A and D. The amplified and compressed pulses duration are respectively 6.7 ps and 495 fs (Lorentz fit) for device A. For MOPA system with SOA D, it shows the similar value, which is 502 fs.

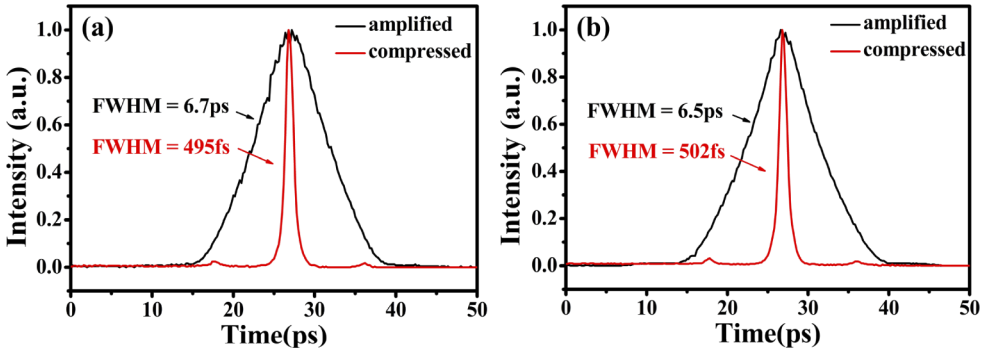

Fig. 7. Autocorrelation trace of the pulse measured after the SOA and pulse compressor for device A (a) and D (b). The corresponding driven current of SOA is 4.6 A.

Figure 8 shows the average power of femtosecond lasers as a function of SOA current for the MOPA system with SOA A and D. The average power is 430 mW for the systme with SOA A at 4.6 A, which is corresponding to a peak power of 1.5 kW. The power roll-over does not occur. Higher driven current does not perform due to the concern of device reliability, where the aging is not carried out for these devices.

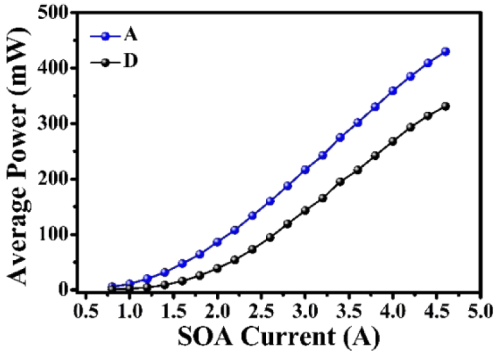

Fig. 8. Average power of the compressed pulses for femtosecond laser A and D as a function of SOA current.

Optics EXPRESS

6. Conclusion

In conclusion, a high peak power femtosecond semiconductor laser based on MOPA system with saw-toothed taper mode-locked laser and amplifier was demonstrated. Comparing with the traditional MOPA system, the innovation in the structure of SOA devices, especially the tilted taper waveguide and saw-toothed edge, decreased evidently the ASE background. The influence of different saw-tooth microstructures in the tapered SOA on the compression of ASE was investigated, and it was found that the saw-tooth microstructures of right- right angled triangle (device A) showed the best effect. The ratio of the maximum intensity to background radiation was increased by 21.9% and the power was increased by 30.5% compared with conventional SOA. The pulse duration of 495 fs and a peak power of 1.5 kW were realized after a double-pass grating compressor. Higher power is expected. We believe that these results will contribute to the development of compact high power all-semiconductor ultrafast laser system**.**

Funding

National Natural Science Foundation of China (61774153, 61761136009); Natural Science Foundation of Jilin Province (20190302053GX, 20180519024JH).

Disclosures

The authors declare no conflicts of interest.

References

1. S. H. Park, D. Y. Yang, and K. S. Lee, "Two-photon stereolithography for realizing ultraprecise three-dimensional nano/microdevices," Laser Photonics Rev. **3**(1-2), 1–11 (2009).
2. K. Sugioka and Y. Cheng, "Ultrafast lasers-reliable tools for advanced materials processing," Light: Sci. Appl. **3**(4), e149 (2014).
3. M. Malinauskas, A. Žukauskas, S. Hasegawa, Y. Hayasaki, V. Mizeikis, R. Buividas, and S. Juodkazis, "Ultrafast laser processing of materials: from science to industry," Light: Sci. Appl. **5**(8), e16133 (2016).
4. S. Toriyama, V. Mizeikis, and A. Ono, "Fabrication of silver nano-rings using photo-reduction induced by femtosecond pulses," Appl. Phys. Express **12**(1), 015004 (2019).
5. Y. Nomura, H. Kawagoe, Y. Hattori, M. Yamanaka, E. Omoda, H. Kataure, Y. Sakakibara, and N. Nishizawa, "Supercontinuum generation for ultrahigh-resolution optical coherence tomography at wavelength of 0.8 μm using carbon nanotube fiber laser and similariton amplifier," Appl. Phys. Express **7**(12), 122703 (2014).
6. M. Yamanaka, H. Kawagoe, and N. Nishizawa, "High-power supercontinuum generation using high-repetition-rate ultrashort-pulse fiber laser for ultrahigh-resolution optical coherence tomography in 1600 nm spectral band," Appl. Phys. Express **9**(2), 022701 (2016).
7. J. Luo, B. Sun, J. Liu, Z. Yan, N. Li, E. L. Tan, Q. Wang, and X. Yu, "Mid-IR supercontinuum pumped by femtosecond pulses from thulium doped all-fiber amplifier," Opt. Express **24**(13), 13939–13945 (2016).
8. S. A. Rezvani, Y. Nomura, K. Ogawa, and T. Fuji, "Generation and characterization of mid-infrared supercontinuum in polarization maintained ZBLAN fibers," Opt. Express **27**(17), 24499–24511 (2019).
9. A. Robertson, M. E. Klein, M. A. Tremont, K. J. Boller, and R. Wallenstein, "2.5-GHz repetition-rate singly resonant optical parametric oscillator synchronously pumped by a mode-locked diode oscillator amplifier system," Opt. Lett. **25**(9), 657–659 (2000).
10. W. Tian, Z. Wang, J. Zhu, and Z. Wei, "Harmonically pumped femtosecond optical parametric oscillator with multi-gigahertz repetition rate," Opt. Express **24**(26), 29814–29821 (2016).
11. E. P. Perillo, J. W. Jarrett, Y. L. Liu, A. Hassan, D. C. Fernée, J. R. Goldak, A. Bonteanu, D. J. Spence, H. C. Yeh, and A. K. Dunn, "Two-color multiphoton in vivo imaging with a femtosecond diamond Raman laser," Light: Sci. Appl. **6**(11), e17095 (2017).
12. C. Lefort, "A review of biomedical multiphoton microscopy and its laser sources," J. Phys. D: Appl. Phys. **50**(42), 423001 (2017).
13. K. Guesmi, L. Abdeladim, S. Tozer, P. Mahou, T. Kumamoto, K. Jurkus, P. Rigaud, K. Loulier, N. Dray, P. Georges, M. Hanna, J. Livet, W. Supatto, E. Beaurepaire, and F. Druon, "Dual-color deep-tissue three-photon microscopy with a multiband infrared laser," Light: Sci. Appl. **7**(1), 12–19 (2018).
14. T. Ulm, F. Harth, H. Fuchs, J. A. Lhuillier, and R. Wallenstein, "InGaAs diode laser system generating pulses of 580 fs duration and 366W peak power," Appl. Phys. B **92**(4), 481–485 (2008).
15. R. Koda, T. Oki, T. Miyajima, H. Watanabe, M. Kuramoto, M. Ikeda, and H. Yokoyama, "100 W peak-power 1 GHz repetition picoseconds optical pulse generation using blue-violet GaInN diode laser mode-locked oscillator and optical amplifier," Appl. Phys. Lett. **97**(2), 021101 (2010).

Optics EXPRESS

16. R. Koda, T. Oki, T. Miyajima, H. Watanabe, S. Konoa, M. Kuramotoa, M. Ikeda, and H. Yokoyama, "High peak power picoseconds optical pulse generation from GaInN semiconductor diode lasers," Proc. SPIE **7953**, 79530J (2011).
17. Y. Ding, R. Aviles-Espinosa, M. A. Cataluna, D. Nikitichev, M. Ruiz, M. Tran, Y. Robert, A. Kapsalis, H. Simos, C. Mesaritakis, T. Xu, P. Bardella, M. Rossetti, I. Krestnikov, D. Livshits, I. Montrosset, D. Syvridis, M. Krakowski, P. Loza-Alvarez, and E. Rafailov, "High peak-power picosecond pulse generation at 1.26 μm using a quantum-dot-based external-cavity mode-locked laser and tapered optical amplifier," Opt. Express **20**(13), 14308–14320 (2012).
18. R. Koda, T. Oki, S. Kono, T. Miyajima, H. Watanabe, M. Kuramoto, M. Ikeda, and H. Yokoyama, "300W peak power picosecond optical pulse generation by blue-violet GaInN mode-locked laser diode and semiconductor optical amplifier," Appl. Phys. Express **5**(2), 022702 (2012).
19. S. Schwertfeger, A. Klehr, T. Hoffmann, A. Liero, H. Wenzel, and G. Erbert, "Picosecond pulses with 50 W peak power and reduced ASE background from an all-semiconductor MOPA system," Appl. Phys. B **103**(3), 603–607 (2011).
20. S. Schwertfeger, A. Klehr, T. Hoffmann, A. Liero, H. Wenzel, and G. Erbert, "Generation of sub-100 ps pulses with a peak power of 65 W by gain switching, pulse shortening, and pulse amplification using a semiconductor-based master oscillator-power amplifier system," Appl. Opt. **52**(14), 3364–3367 (2013).
21. Y. Wang, X. Zhang, C. Tong, L. Wang, S. Shu, and L. Wang, "Harmonic mode-locking in an external cavity tapered diode laser with saw-toothed microstructure," Appl. Phys. Express **12**(10), 102011 (2019).
22. T. Wang, C. Tong, L. Wang, Y. Zeng, S. Tian, S. Shu, J. Zhang, and L. Wang, "Injection-insensitive lateral divergence in broad-area diode lasers achieved by spatial current modulation," Appl. Phys. Express **9**(11), 112102 (2016).
23. T. Ulma, F. Hartha, A. Klehrb, G. Erbertb, and J. Lhuillier, "Passively mode-locked 1 GHz MOPA system generating sub-500-fs pulses after external compression," Proc. SPIE **8432**, 84320Y (2012).
24. J.-C. Diels and W. Rudolph, "*Ultrashort Laser Pulse Phenomena*," (Academic, Amsterdam, 2006).